

X-651-73-319

PREPRINT

NASA TM X- 70497

A SEARCH FOR GLOBAL AND SEASONAL VARIATION OF METHANE FROM NIMBUS 4 IRIS MEASUREMENTS

C. PRABHAKARA
G. DALU
V. G. KUNDE

OCTOBER 1973



GODDARD SPACE FLIGHT CENTER
GREENBELT, MARYLAND

(NASA-TM-X-70497) A SEARCH FOR GLOBAL AND SEASONAL VARIATION OF METHANE FROM NIMBUS 4 IRIS MEASUREMENTS (NASA) 29 p HC \$3.50 CSCL 00A

N74-10368

Unclas
21567

G3/13

A SEARCH FOR GLOBAL AND SEASONAL VARIATION OF
METHANE FROM NIMBUS 4 IRIS MEASUREMENTS

C. Prabhakara

G. Dalu

V. G. Kunde

October 1973

GODDARD SPACE FLIGHT CENTER
Greenbelt, Maryland

/

PRECEDING PAGE BLANK NOT FILMED

A SEARCH FOR GLOBAL AND SEASONAL VARIATION OF
METHANE FROM NIMBUS 4 IRIS MEASUREMENTS

C. Prabhakara, G. Dalu* and V. G. Kunde

ABSTRACT

The Nimbus 4 Infrared Interferometer Spectrometer (IRIS) measurements in the region around 1304 cm^{-1} show absorption due to methane in the earth's atmosphere.

From the laboratory measurements of the absorption coefficient and a selected vertical distribution corresponding to 1.13 atm cm of methane, a theoretical model for the transmittance at 1304 cm^{-1} is developed. The weighting function deduced from this model shows a maximum around 300 mb . Some weak absorption due to nitrous oxide (N_2O) in the atmosphere has been taken into account.

The vertical temperature profile, derived from the $15\text{ }\mu\text{m}$ CO_2 band in the IRIS spectrum, together with the methane weighting function have been used in a consistent way to compute the upwelling intensity at 1304 cm^{-1} . The brightness temperature corresponding to the IRIS observed radiance at 1304 cm^{-1} has been compared with the brightness temperature deduced from the calculated upwelling

*NRC—Research Associate. Permanent address: C.N.R.—Istituto di Fisica dell'Atmosfera—Rome, Italy.

intensity from 80° North to 80° South and for different periods of the year. This comparison shows that the two brightness temperatures agree with one another to within the accuracy of measurements, about 2°K and that their difference reveals no geographic pattern. An error of 2°K in brightness temperature, relates to an error of 0.25 atm cm of methane. From this result we find that global or seasonal variability of methane is less than ± 0.25 atm cm.

CONTENTS

	<u>Page</u>
ABSTRACT	iii
INTRODUCTION	1
DESCRIPTION OF SPECTRA	2
METHOD	7
RESULTS	11
CONCLUSIONS	15
ACKNOWLEDGMENTS	16
REFERENCES	16
APPENDIX A—Statistical Band Model Parameters for CH ₄ and N ₂ O	A-1

ILLUSTRATIONS

<u>Figure</u>		<u>Page</u>
1	Observed IRIS Spectrum and the Computed Spectrum Including Only Water Vapour Absorption	4
2	Absorption Spectra for Methane and Nitrous Oxide, and the Residual Spectrum ΔT	6
3	Weighting Functions for Methane and Nitrous Oxide at 1304 cm ⁻¹	10
4	Difference Between the Computed and the Observed Brightness Temperatures at 1304 cm ⁻¹	12
5	Comparison Between the Observed and the Calculated Brightness Temperatures	14

A SEARCH FOR GLOBAL AND SEASONAL VARIATION OF
METHANE FROM NIMBUS 4 IRIS MEASUREMENTS

INTRODUCTION

Methane is present in the earth's atmosphere as a minor constituent (Migeotte, 1948). Measurements of the total amount of methane and its vertical distribution derived from balloon and rocket flights (Ehhalt and Heidt, 1973; For short summary see Drayson et al., 1972, and also Friend, 1972) indicate the mixing ratio of methane in the atmospheric layers near the surface changes from about 0.6 to 2.0 ppm by volume. In the troposphere this gas appears to be well mixed with a mixing ratio of about 1.41 ppm. Above the tropopause the mixing ratio decreases reaching a value of ~ 0.25 ppm near 50 km altitude. The total amount of the gas per unit area corresponding to an average mixing ratio of 1.41 ppm is about 1.13 atm cm.

The main source of methane is on land from the decomposition of organic matter (Koyama, 1963) with no known sources in the atmosphere. Atmospheric photochemical investigations suggest oxidation of methane as a sink, both in the troposphere (Weinstock and Nicki, 1972) and in the stratosphere (McConnell et al., 1972, Wofsy, et al., 1972). Because methane is produced on land, a variation with geographic location, or at least an asymmetry between the northern and southern hemisphere would be expected. However, the mean atmospheric residence times of 1-7 years derived from photochemical theories (Weinstock and Nicki, 1972; Wofsy,

et al., 1972; Junge, 1972; Wofsy and McElroy, 1973) should be sufficiently long to smooth out any source variations and distribute the gas uniformly over the globe.

The available measurements on methane concentration, made with different measuring techniques and confined to limited geographic regions, are not sufficient to present a comprehensive picture of the temporal and spatial variation of methane in the earth's atmosphere. Remote sensing satellite instruments are ideally suited to examine the large scale variability of methane. Measurements made by the Infrared Interferometer Spectrometer (IRIS), aboard the Nimbus 3 and Nimbus 4 satellites, clearly show the absorption features produced by methane in the atmosphere in the $1225\text{-}1325\text{ cm}^{-1}$ region (Conrath et al., 1970; Hanel and Conrath, 1970). These satellite measurements covered the globe from 80°N to 80°S and in the case of Nimbus 4 satellite were available for about one year.

In this investigation the Nimbus IV IRIS spectra have been examined for any global or seasonal deviations of methane from its mean value of 1.41 ppm.

DESCRIPTION OF SPECTRA

The Infrared Interferometer Spectrometer (IRIS) measured the thermal emission of the earth's atmosphere and surface from $400\text{-}1600\text{ cm}^{-1}$ with an apodized spectral resolution of 2.8 cm^{-1} . The instrument and its performance have been described by Hanel, et al., 1972, together with the instrumental calibration and an overview of some observed spectra. The radiometric precision of the instrument

is high with the noise equivalent radiance (NER) of $\sim 0.5 \text{ erg sec}^{-1} \text{ cm}^{-2} \text{ sr}^{-1} / \text{cm}^{-1}$ as estimated from the in-flight calibration.

Absorption features of ν_4 fundamental vibration rotation band of methane have been observed in the $1225\text{-}1325 \text{ cm}^{-1}$ region of the IRIS spectra. This band has a narrow Q-branch with intense absorption around 1304 cm^{-1} . An observed brightness temperature spectrum of IRIS, in the $1200\text{-}1350 \text{ cm}^{-1}$ region, taken over the Pacific ocean near Guam on April 27, 1970 is shown in Figure 1 to illustrate this strong feature. This spectral feature is easily noticeable in the IRIS spectra taken over the globe from 80° N to 80° S .

From an examination of the observed brightness temperature spectrum in Figure 1 one can readily notice the presence of several lines of water vapour superimposed on the methane band. To appreciate quantitatively the water vapour interference a theoretical spectrum resulting purely from water vapour absorption is calculated with the help of temperature and relative humidity measurements made by a radio-sonde at Guam. Detailed line by line direct integration slant path program is used for this purpose. The theoretical brightness temperature spectrum obtained from such a calculation is shown in Figure 1. From a comparison of these two spectra one can see that the spectral region $1200\text{-}1350 \text{ cm}^{-1}$ is profoundly influenced by the water vapour lines with the exception of several narrow water vapour windows. The presence of one water vapour window particularly at 1300 cm^{-1} favours the Q-branch of the CH_4 band to manifest itself in the IRIS spectra.

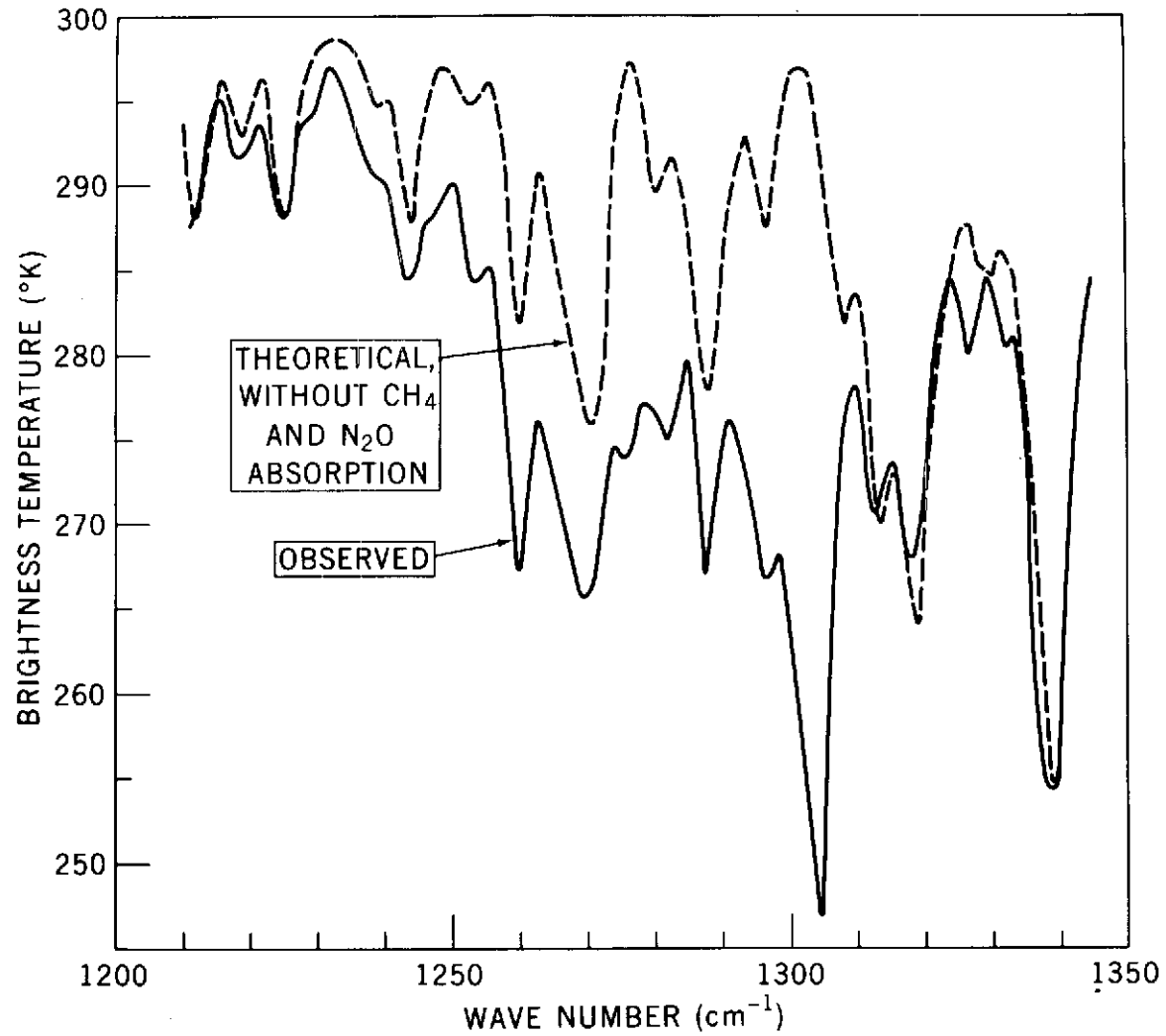


Figure 1. Observed IRIS Spectrum and the Computed Spectrum Including Only Water Vapour Absorption

The water vapour absorption in the observed spectrum can be eliminated by taking the difference between the two brightness temperature spectra shown in Figure 1. This difference or "residual" spectrum ΔT , as shown in Figure 2, can then be examined for many absorption features that are weaker than the Q-branch of CH_4 . In the spectral region $1200\text{--}1350\text{ cm}^{-1}$ the ν_1 band of N_2O , another known minor constituent of the atmosphere, also produces absorption. For this reason the CH_4 and N_2O features in the residual spectrum are scrutinized with the help of the absorption bands of these two gases which are included in Figure 2. These absorption bands are calculated with the band model parameters described in Appendix A. To simulate the atmospheric conditions in these calculations the pressure is taken as 500 mb, and the assumed CH_4 and N_2O path lengths are 1.13 cm and 0.25 cm respectively.

In the methane ν_4 fundamental band the rotational lines for each rotational quantum number (J) of the P- and R-branches are spaced $\sim 5\text{ cm}^{-1}$ apart. A general correspondence between the calculated methane band and the residual spectrum (see Fig. 2) is evident. The P- and R-branches of the ν_1 band of N_2O produce absorption peaks at 1276 and 1304 cm^{-1} respectively. The residual spectrum also reflects the presence of these features. As the mean line spacing of N_2O is $\sim 0.8\text{ cm}^{-1}$ individual N_2O lines are not identifiable in the spectrum.

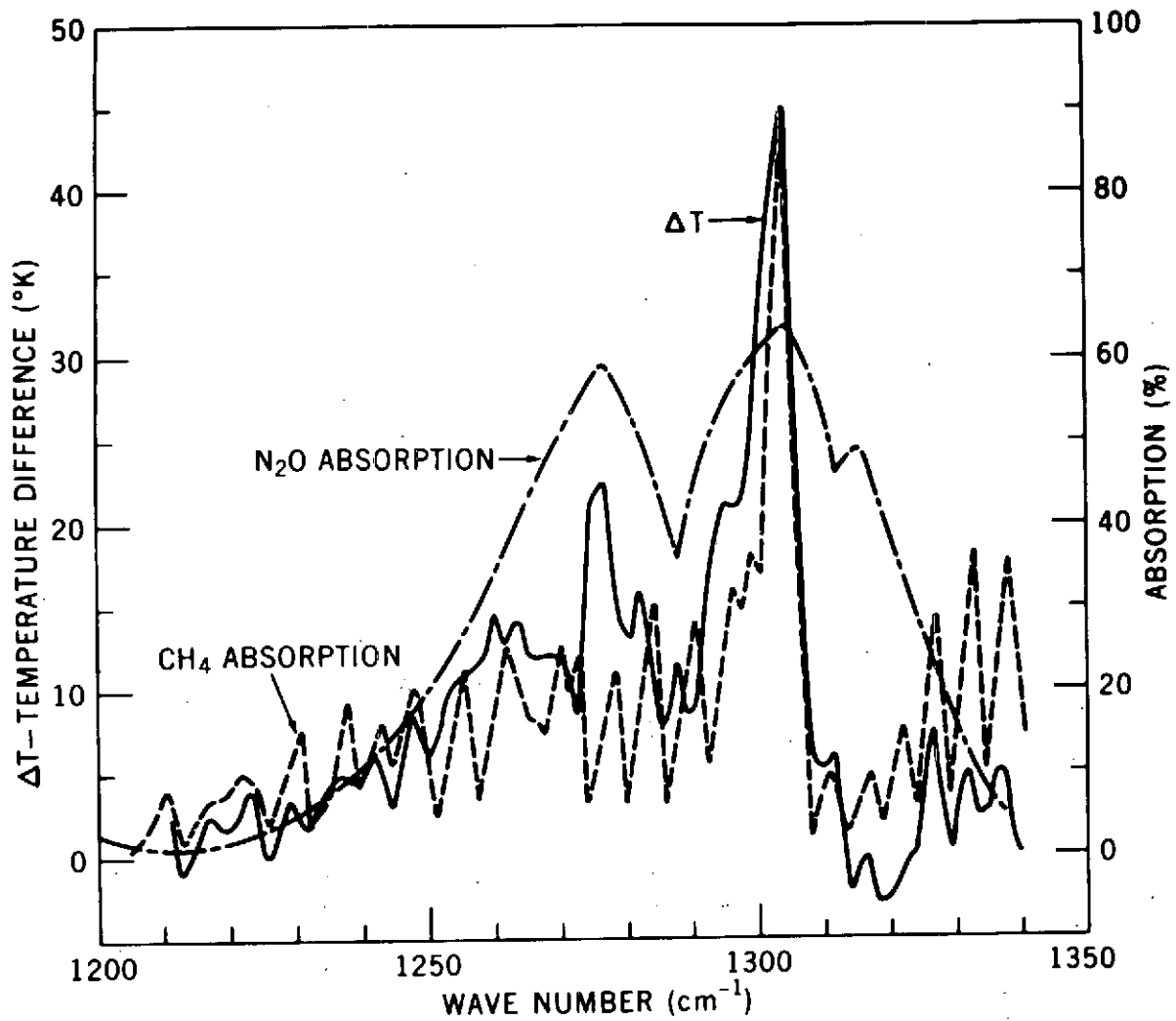


Figure 2. Absorption Spectra for Methane and Nitrous Oxide, and the Residual Spectrum ΔT

METHOD

Remote sensing of a minor gaseous constituent in the earth's atmosphere, from thermal infrared measurements, is feasible when that gas produces measurable absorption. It is, however, necessary to have simultaneously a temperature sounding of the atmosphere to make a quantitative estimate of the amount of the gas. In addition, if we wish to measure the global or seasonal variability of the gas with a meaningful accuracy, the absorption due to other variable atmospheric gases, particularly the water vapour, should not adversely interfere. Success in remote sensing of the global distribution of ozone (Prabhakara, et al., 1970), from the $9.6\mu\text{m}$ IRIS measurements, in the presence of some water vapour absorption supports this point of view.

In this study, we make an estimation of the CH_4 amount from the 1304 cm^{-1} Q-branch feature. A radiative transfer model is developed for this purpose.

From the radiative transfer formalism, in a non-scattering atmosphere under local thermodynamic equilibrium we can relate the upwelling intensity $I(\nu)$ as

$$I(\nu) = B(\nu, T(p_0)) \tau(\nu, p_0) + \int_{\tau(\nu, p_0)}^1 B(\nu, T(p)) d\tau(\nu, p) \quad (1)$$

where p_0 and p are surface pressure and pressure at any height (mb),

ν is the wave number (cm^{-1}),

T is the temperature (K),

B is the Planck intensity,

τ is the transmission from any pressure level p to the top of the atmosphere.

The temperature sounding $T(p)$ needed in Equation 1 is obtained by performing an inversion of the IRIS measurements in the 667 cm^{-1} CO_2 band (Conrath, et al., 1972). The transmission function $\tau = \tau_{\text{N}_2\text{O}} * \tau_{\text{CH}_4}$ is calculated with the band model parameters of CH_4 and N_2O given in Appendix A. For the purpose of these calculations, it is assumed that in the lower atmosphere up to about 100 mb CH_4 has a constant mixing ratio of 1.41 ppm and above 100 mb the mixing ratio decreases linearly with respect to height to 0.25 ppm at 50 km level (Ehhalt and Heidt, 1973). N_2O is assumed to be uniformly mixed with a mixing ratio of 0.3 ppm. In Table 1 the distribution of the gases and the calculated transmission functions for 1304 cm^{-1} are tabulated.

In Figure 3 the weighting function, $d\tau/d\ln p$ for each gas and for both gases is shown. The emission of N_2O primarily originates from the lowest layers in the atmosphere where the water vapour is present. Water vapour absorption, although weak, can range from a maximum of about 50% in the tropics to less than 20% at high latitudes. Thus the N_2O information at 1304 cm^{-1} is damaged by water vapour absorption. At 1276 cm^{-1} , atmospheric N_2O has about the same absorption as that at 1304 cm^{-1} (see Table 1) and so the weighting function for N_2O in this spectral region also has a maximum near the surface. The water vapour absorption in the lower atmosphere precludes the possibility of measuring N_2O either from 1304 or from 1276 cm^{-1} . For this reason we have

Table 1

Pressure (mb)	CH ₄ Path Length (atm cm)	N ₂ O Path Length (atm cm)	CH ₄ Trans- missivity at 1304 cm ⁻¹	N ₂ O Trans- missivity at 1304 cm ⁻¹	Total Transmissivity at 1304 cm ⁻¹	Total Transmissivity at 1276 cm ⁻¹	Height (km)
3.7	0.0011	0.0009	0.995	0.996	0.992	0.996	38.2
5.5	0.0023	0.0014	0.992	0.994	0.987	0.994	35.2
8.2	0.0045	0.0020	0.987	0.992	0.979	0.991	32.6
12.2	0.0081	0.0030	0.979	0.988	0.967	0.987	29.9
18.2	0.0143	0.0045	0.967	0.981	0.949	0.980	27.2
27.2	0.0244	0.0068	0.947	0.972	0.921	0.969	24.6
40.5	0.0410	0.0101	0.918	0.959	0.881	0.954	22.0
60.5	0.0683	0.0151	0.877	0.940	0.824	0.932	19.4
90.4	0.1020	0.0226	0.822	0.911	0.750	0.900	16.9
134.9	0.1520	0.0337	0.747	0.871	0.650	0.855	14.3
201.4	0.2280	0.0503	0.647	0.813	0.526	0.791	11.8
300.6	0.3400	0.0751	0.522	0.734	0.383	0.705	9.1
448.8	0.5070	0.1120	0.379	0.631	0.239	0.593	6.4
669.9	0.7570	0.1670	0.235	0.503	0.118	0.458	3.3
1000.0	1.1300	0.2500	0.115	0.358	0.041	0.312	0.1

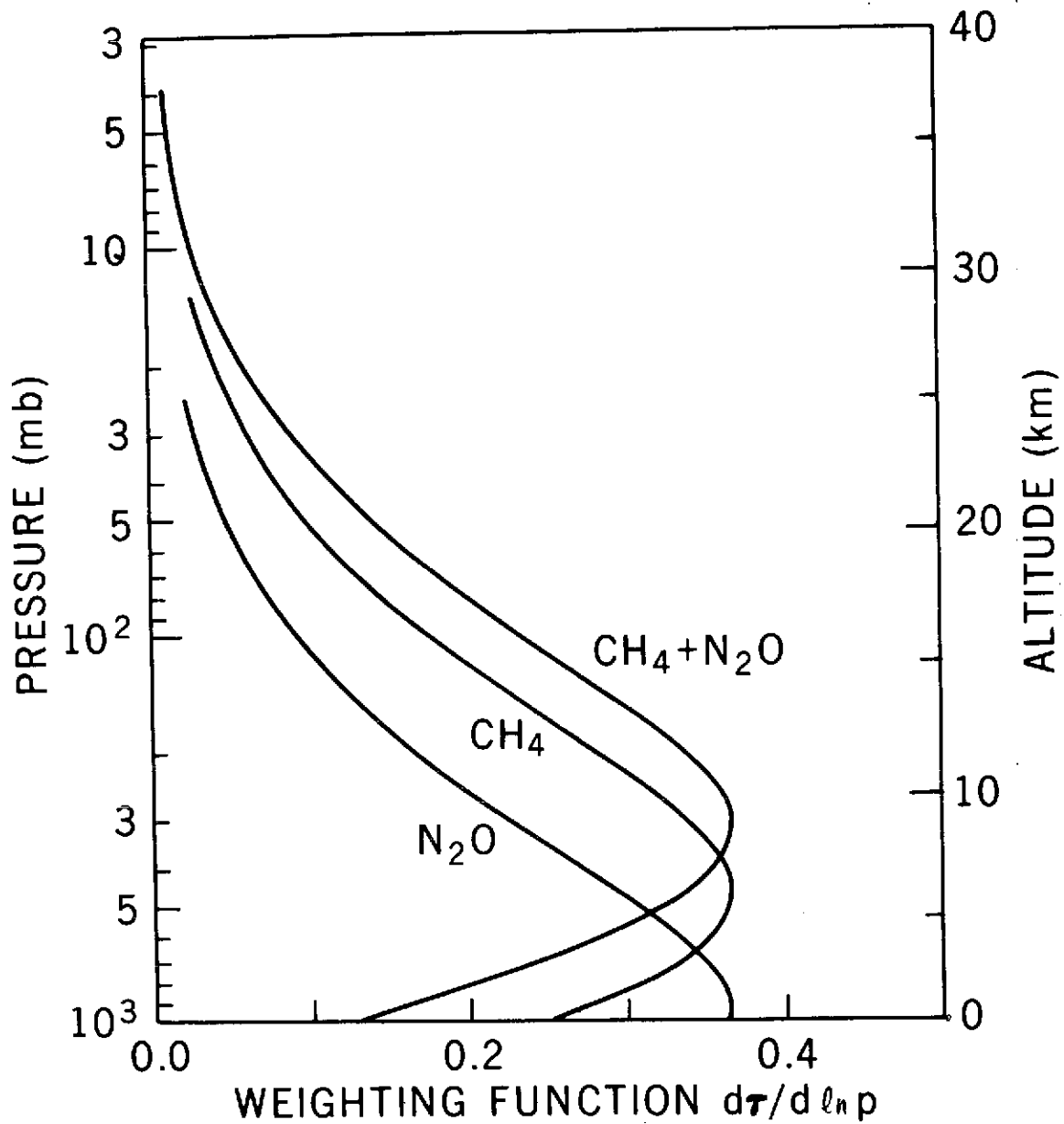


Figure 3. Weighting Functions for Methane and Nitrous Oxide at 1304 cm^{-1}

assumed the mixing ratio of N_2O in the atmosphere is 0.3 ppm (corresponding to 0.25 atm cm) invariable with respect to time and geographic location. However, large part of the methane information originates around 450 mb as can be seen from Figure 3, which is considerably separated from the water vapour in the lower atmosphere. Thus the 1304 cm^{-1} measurements can yield some information about methane.

In the present study the spectral measurements at 1304 cm^{-1} are examined for deviations of CH_4 from the global mean value of 1.13 cm atm in the following fashion. Synthetic radiances are computed at 1304 cm^{-1} from Equation 1, using $T(p)$ from the inversion of the 667 cm^{-1} CO_2 band. The CH_4 and N_2O transmission functions (see Table 1) used in these calculations correspond to the total amounts of 1.13 and 0.25 cm atm, respectively. The 1304 cm^{-1} calculated radiance and the corresponding brightness temperature are compared with the IRIS observed data. The difference between the observed and calculated brightness temperatures can be related to the deviation of methane amount from its global mean.

RESULTS

The difference in the observed and computed brightness temperature, δT , is shown in Figure 4 for orbit 1207, July 7, 1970, going from 80°N to 80°S . The δT shown has a standard deviation of 2.5°K and reveals no latitudinally dependent variation. The data corresponding to large δT are associated with high clouds.

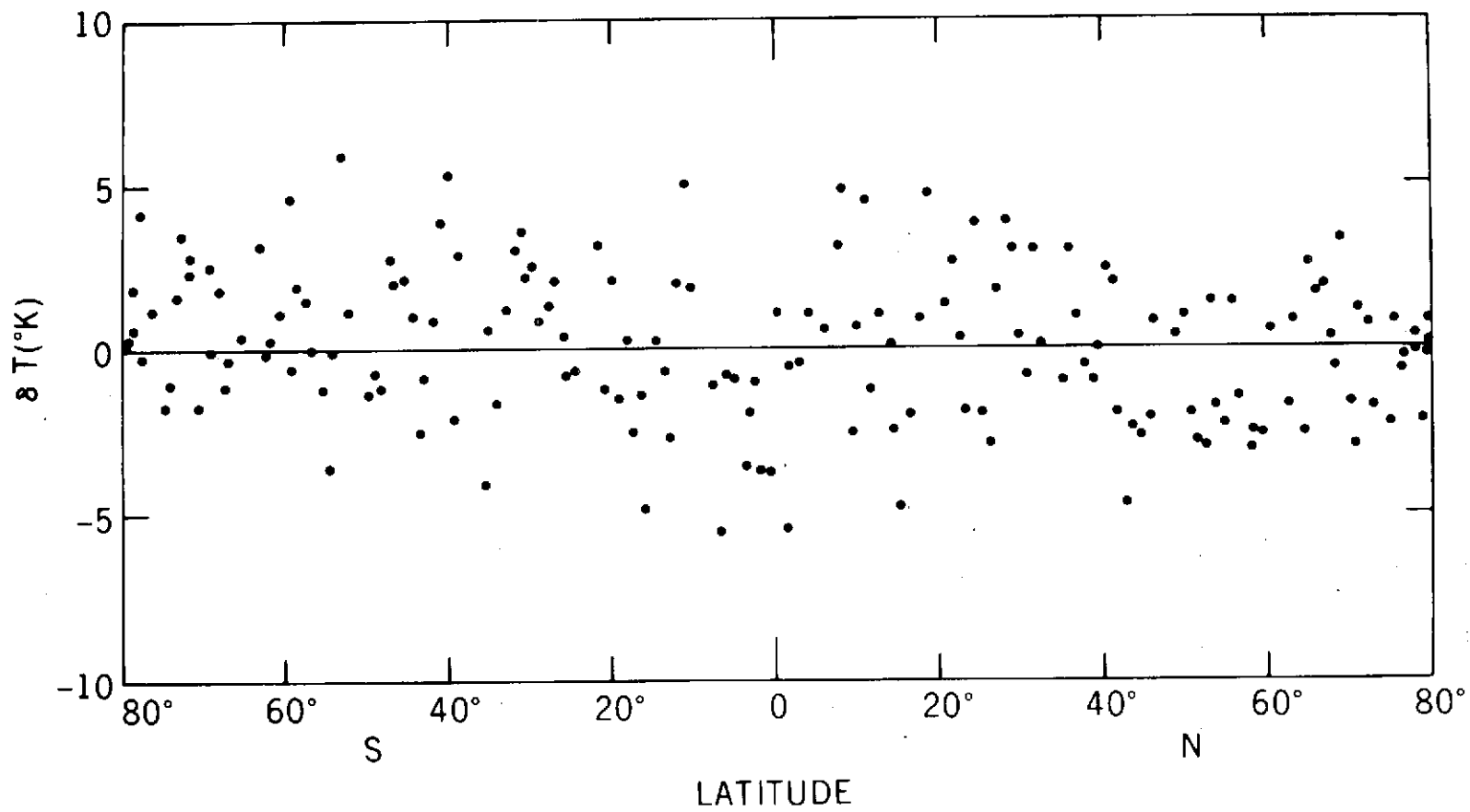


Figure 4. Difference Between the Computed and the Observed Brightness Temperatures at 1304 cm⁻¹

The $15\mu\text{m}$ CO_2 temperature soundings derived from spectra contaminated by high clouds are in considerable error and so are the upwelling intensities calculated at 1304 cm^{-1} using such temperature data. However, when the clouds are at lower levels in the atmosphere these errors are reduced.

In further analysis of IRIS data we have eliminated high cold cloud contaminated spectra. These high cold clouds can be easily identified from the 900 cm^{-1} ($11\mu\text{m}$) IRIS window measurements. When the high altitude cloud contaminated data are not considered the δT shown in Figure 4 has a standard deviation of about 2°K . This error is comparable to the noise equivalent temperature (NET) of IRIS measurements at 1304 cm^{-1} . The model calculations indicate that in order to change the brightness temperature by $\pm 2^\circ\text{K}$ the mixing ratio of methane should be changed by ± 0.25 ppm. This result implies the sensitivity in measuring CH_4 from IRIS data is about $\pm 25\%$ of the global mean value.

With this technique we have processed Nimbus 4 IRIS data to examine if there are any organized patterns in δT over the globe on a daily or monthly mean basis. We find from this study that there are no organized patterns in methane distribution.

These results can be demonstrated from the scatter diagram shown in Figure 5 where the calculated brightness temperature and the observed brightness temperature at 1304 cm^{-1} are plotted for different geographic areas and for different seasons. The brightness temperatures range from 225°K near the polar regions to 255°K in the tropics. If the calculated and observed brightness

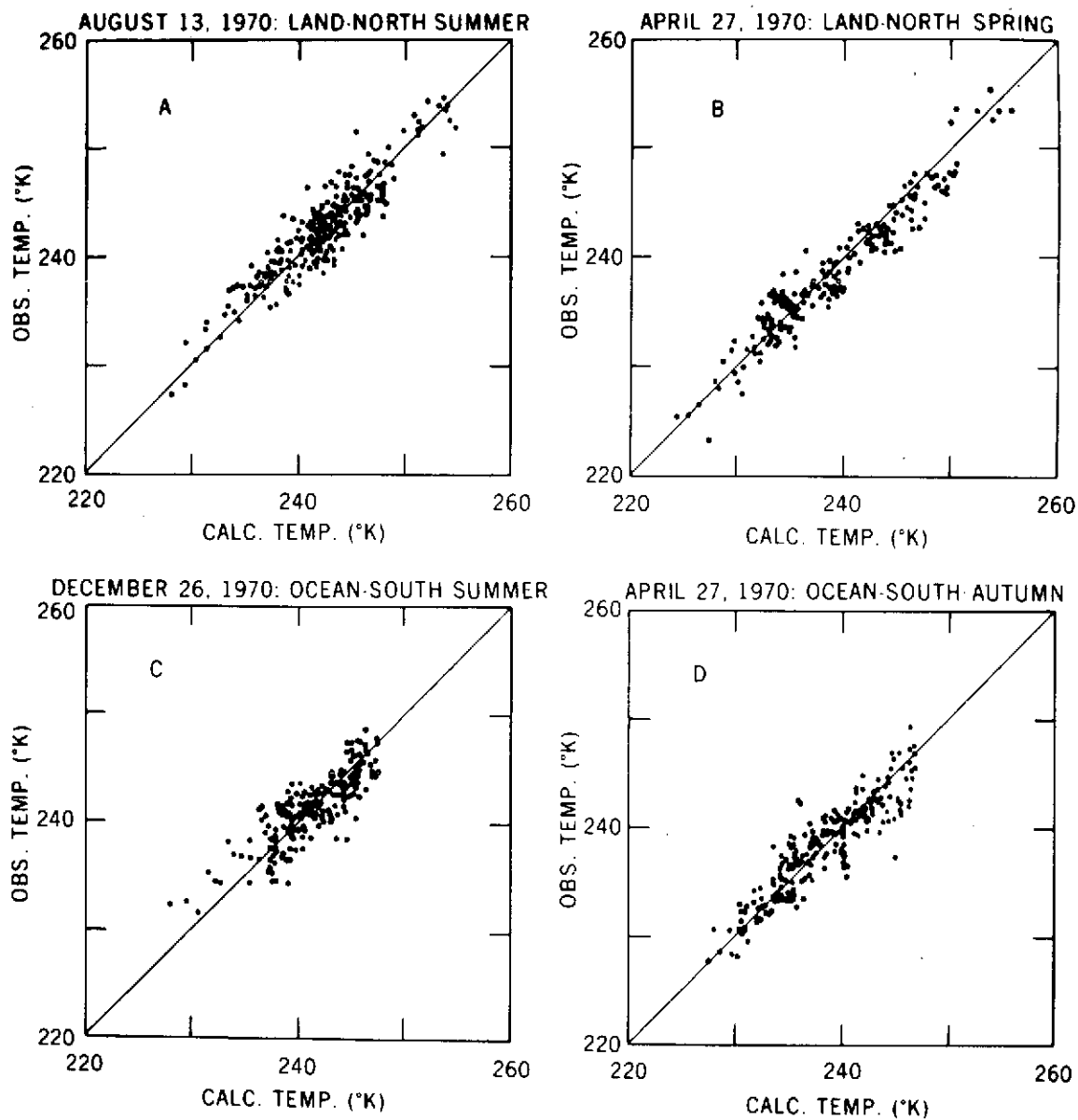


Figure 5. Comparison Between the Observed and the Calculated Brightness Temperatures

temperatures are equal the data points in Figure 5 should fall on the line having 45° slope. If there is more methane than 1.13 atm cm, we should find the observed brightness temperature systematically colder than the calculated one. From Figure 5a and 5b, representing the variability of methane over land, we see the data closely follows the line having 45° slope. Similar results are found from the oceanic cases shown in Figure 5c and 5d.

The standard deviation of the data in all these cases with respect to the 45° line is about 2° K. Further in all these cases the scatter of the data does not suggest any systematic increase or decrease in mixing ratio with respect to latitude or season.

CONCLUSIONS

In the present study, information on the global distribution of methane from a satellite is obtained for the first time. The results obtained over the land, where the sources of methane are present, show no appreciable differences from the results obtained over the ocean. Also no seasonal variation has been detected. From this study it can be stated that there is no global or seasonal variability of methane to within an accuracy of 0.25 ppm. This suggests that methane has a life time long enough to produce a uniform global distribution.

Remote measurements at high spectral resolution ($\sim 0.1 \text{ cm}^{-1}$), which can isolate the absorption features of H_2O , CH_4 and N_2O , would permit one to

measure the global and seasonal variability of CH_4 , with an accuracy better than the ± 0.25 ppm limits set by the Nimbus 4 IRIS measurements. Additionally the higher spectral resolution may be useful in the determination of the vertical distribution of CH_4 and the total amount of N_2O .

ACKNOWLEDGMENTS

The authors are grateful to Drs. R. A. Hanel, B. J. Conrath, R. Wexler for their constructive criticism and comments.

REFERENCES

- Blaine, R. L. and W. A. Hovis, Private Communication, NASA-GSFC, Greenbelt, 1973.
- Burch, D. E., D. A. Gryvnak, E. B. Singleton, W. L. France, and D. Williams, Infrared Absorption by CO_2 , Water Vapour, and Minor Atmospheric Constituents - AFCRL - 62 - 698, Air Force Cambridge Res. Labs., 1962.
- Conrath, B. J., R. A. Hanel, V. G. Kunde, and C. Prabhakara, The Infrared Interferometer Experiment on Nimbus 3, *J. Geophys. Res.*, 75, 5831-5857, 1970.
- Conrath, B. J., Vertical Resolution of Temperature Profiles Obtained from Remote Radiation Measurements, *J. Atmos. Sci.*, 29, 1262-1271, 1972.

- Drayson, S. R., F. L. Bartman, W. R. Kuhn, and R. Tallamraju, Satellite Measurement of Stratospheric Pollutants and Minor Constituents by Solar Occultation: A Preliminary Report, The University of Michigan, Report 011023 - 1 - T, 1972.
- Ehhalt, D. H. and L. E. Heidt, Vertical Profiles of CH₄ in the Troposphere and Stratosphere, J. Geophys. Res., 78, 5265-5271, 1973.
- Friend, J. P., Trace material composition of the lower stratosphere, Climatic Impact Assessment Program, Proceedings of the Survey Conference, DOT - TSC - OST - 72 - 73, 1972.
- Goody, R. M. and T. W. Wormell, The quantitative determination of atmospheric gases by infrared spectroscopic methods, Royal Society of London, Proceedings, 209, 178-196, 1951.
- Goody, R. M., Atmospheric Radiation I. Theoretical Basis, Oxford, Clarendon Press, 1964.
- Hanel, R. A. and B. J. Conrath, Thermal Emission Spectra of the Earth and Atmosphere from the Nimbus 4 Michelson Interferometer Experiment, Nature, 228, 143-145, 1970.
- Hanel, R. A., B. J. Conrath, V. G. Kunde, C. Prabhakara, I. Revah, V. V. Salomonson, and G. Wolford, The Nimbus 4 Infrared Spectroscopy Experiment, J. Geophys. Res., 77, 2629-2641, 1972.

- Junge, C., The cycle of atmospheric gases - natural and man made, Quart. J. R. Met. Soc., 98, 711-729, 1972.
- Koyama, T., Gaseous Metabolism in Lake Sediments and Paddy Soils and the Production of Atmospheric Methane and Hydrogen, J. Geophys. Res., 68, 3971-3973, 1963.
- McConnell, J. C., M. B. McElroy, and S. C. Wofsy, Natural sources of atmospheric CO, Nature, 233, 187-188, 1972.
- Migeotte, M., Methane in the earth's atmosphere, Astrophys. J., 107, 400-403, 1948.
- Nielsen, A. H. and H. H. Nielsen, The Infrared Absorption Bands of Methane, Physical Review, 48, 864-867, 1935.
- Prabhakara, C., B. J. Conrath, R. A. Hanel, and E. J. Williamson, Remote Sensing of Atmospheric Ozone Using the $9.6\mu\text{m}$ Band, Jour. of Atm. Sciences, 27, 689-697, 1970.
- Varanasi, P. and G. D. T. Tejwani, Experimental and Theoretical Studies on Collision - Broadened lines in the ν_4 - Fundamental of Methane, J. Q.S.R. T., 12, 849-855, 1972.
- Weinstock, B. and R. Nicki, Carbon monoxide in nature, Science, 176, 290-292, 1972.

Wofsy, S. C., J. C. McConnell, and M. B. McElroy, Atmospheric CH₄, CO, and CO₂, J. Geophys. Res., 77, 4477-4493, 1972.

Wofsy, S. C. and M. B. McElroy, On vertical mixing in the upper stratosphere and lower mesosphere, J. Geophys. Res., 78, 2619-2624, 1973.

LIST OF ILLUSTRATIONS

- Figure 1. Observed IRIS Spectrum and the Computed Spectrum Including Only Water Vapour Absorption
- Figure 2. Absorption Spectra for Methane and Nitrous Oxide, and the Residual Spectrum ΔT
- Figure 3. Weighting Functions for Methane and Nitrous Oxide at 1304 cm^{-1}
- Figure 4. Difference Between the Computed and the Observed Brightness Temperatures at 1304 cm^{-1}
- Figure 5. Comparison Between the Observed and the Calculated Brightness Temperatures

APPENDIX A

STATISTICAL BAND MODEL PARAMETERS FOR CH₄ AND N₂O

APPENDIX A

STATISTICAL BAND MODEL PARAMETERS FOR CH₄ AND N₂O

The absorption bands of methane and N₂O of relevance to the present study have been investigated among others by Burch et al., 1962, in the laboratory for several path lengths and pressures. Their measurements were made with a spectral resolution of about 10 cm⁻¹ which is crude for the purpose of explaining the IRIS spectra having a resolution of 2.8 cm⁻¹. Absorption spectra in our laboratory were obtained (Blaine and Hovis, 1973) for CH₄ and N₂O with a resolution of 2.8 cm⁻¹. With the help of both these sets of data we are able to fit the absorption bands of CH₄ and N₂O to a statistical band model (Goody, 1964). The band model permits us to express the transmission τ as

$$\tau = \text{Exp} \left[-kw \left(1 + \frac{kw}{4 \alpha_0 / \delta p/p_0} \right)^{-1/2} \right] \quad (\text{A1})$$

where k is the absorption coefficient (atm⁻¹ cm⁻¹),

w is the absorber path (atm cm),

α_0 is the line half width at STP (cm⁻¹ atm⁻¹),

δ is the average line spacing (cm⁻¹),

p is the pressure and p_0 the standard pressure (mb).

The various band model parameters that have been used to compute CH₄ and N₂O spectrum are listed in Tables A-1 and A-2.

Table A-1

Wave number (cm^{-1})	METHANE		NITROUS OXIDE	
	Absorption coefficient ($\text{atm}^{-1} \text{cm}^{-1}$)	Absorption for 1.1 atm cm of methane at a pressure of 0.5 atm	Absorption coefficient ($\text{atm}^{-1} \text{cm}^{-1}$)	Absorption for 0.25 atm cm of nitrous oxide at a pressure of 0.5 atm
1210.6	0.23	0.078	0.018	0.012
1213.0	0.01	0.016	0.018	0.012
1222.0	0.36	0.100	0.100	0.023
1226.0	0.04	0.040	0.145	0.035
1231.0	0.85	0.153	0.230	0.054
1234.4	0.04	0.038	0.240	0.066
1238.0	1.32	0.184	0.430	0.088
1239.6	0.20	0.085	0.480	0.100
1243.2	0.92	0.160	0.670	0.127
1244.5	0.46	0.110	0.740	0.140
1248.0	1.54	0.200	1.040	0.175
1251.5	0.09	0.050	1.320	0.215
1255.5	2.02	0.225	1.940	0.270
1257.5	0.17	0.066	2.280	0.300
1262.0	2.62	0.250	3.360	0.372
1267.5	0.80	0.147	5.450	0.465
1270.0	2.62	0.250	6.620	0.503
1271.3	1.50	0.198	7.200	0.520
1273.0	2.42	0.240	8.350	0.548
1274.0	0.15	0.062	8.600	0.558
1276.5	0.85	0.152	9.900	0.588
1278.5	2.00	0.220	8.720	0.560
1280.0	0.14	0.060	7.800	0.537
1284.6	4.03	0.302	5.200	0.455
1286.0	0.14	0.060	4.300	0.417
1290.5	3.41	0.280	5.050	0.448
1292.5	0.46	0.110	6.350	0.494
1296.2	4.51	0.318	8.600	0.554
1297.5	3.89	0.296	9.000	0.568
1299.0	6.21	0.362	10.000	0.590
1300.5	5.41	0.342	11.000	0.606
1304.3	138.00	0.880	13.000	0.640
1308.2	0.01	0.022	9.700	0.582
1311.0	0.33	0.096	6.850	0.510
1313.5	0.02	0.026	5.800	0.478
1317.0	0.33	0.095	5.450	0.465
1322.0	0.83	0.151	3.100	0.352
1324.0	0.14	0.060	2.280	0.300

Table A-1 (Continued)

Wave number (cm^{-1})	METHANE		NITROUS OXIDE	
	Absorption coefficient ($\text{atm}^{-1} \text{cm}^{-1}$)	Absorption for 1.1 atm cm of methane at a pressure of 0.5 atm	Absorption coefficient ($\text{atm}^{-1} \text{cm}^{-1}$)	Absorption for 0.25 atm cm of nitrous oxide at a pressure of 0.5 atm
1327.0	3.62	0.287	1.440	0.225
1329.0	0.20	0.068	1.040	0.178
1333.0	6.44	0.366	0.520	0.105
1334.5	0.36	0.100	0.400	0.082
1338.0	5.98	0.358	0.190	0.045
1340.5	0.74	0.141	0.100	0.025

Table A-2

METHANE		NITROUS OXIDE	
α_0	= 0.085 atm (Varanasi and Tejwani, 1972)	α_0	= 0.152 atm (Goody and Wormell, 1951)
δ	= 5.8 cm^{-1} (Nielsen and Nielsen, 1935)	δ	= 0.836 cm^{-1} (Goody and Wormell, 1951)
α_0/δ	= 0.015 atm cm (Adopted value)	α_0/δ	= 0.18 atm cm (Adopted value)